

Morphology control in the bulk heterojunction blend of inverted organic solar cell via co-solvent addition

Sarita S Nair, D Kumar*

Department of Applied Chemistry & Polymer Technology, Delhi Technological University, (Formerly Delhi College of Engineering), Shahbad Daulatpur, Bawana Road, Delhi 110042, India

*Corresponding author. Tel: (+91) 9811425817; E-mail: dkumar@dce.ac.in; drdkumar@yahoo.co.uk

Received: 07 October 2015, Revised: 08 February 2016 and Accepted: 25 May 2016

ABSTRACT

This work is supposed to expand the concept of solvent induced crystallisation of donor poly(3-hexylthiophene) (P3HT) polymer, to the photoactive blend of inverted organic solar cells. With the optimised concentration of cyclohexanone (CHN) co-solvent and ageing period of 2 h for the active layer precursor solution, the power conversion efficiency of a typical device increased to 3.09% compared with 2.77% efficiency achieved in a similar kind of inverted device without CHN modification. This improvement of 10% in the efficiency of inverted device with CHN addition was related to the increased current density and fill factor of the device. Increased P3HT crystallinity for efficient photo-absorption and commensurate vertical concentration gradient observed in the P3HT fractions of the blend for efficient hole transport is possibly responsible for the betterment of the photovoltaic parameters in the modified device. Copyright © 2016 VBRI Press.

Keywords: Crystallisation; morphology; inverted organic solar cell; non-solvent.

Introduction

The advent of bulk heterojunction (BHJ) concept in the photoactive layer composed of conjugated polymer donor and soluble fullerene acceptor extends the advantage of thicker photoactive layer implementation in organic solar cells (OSCs). And, unlike their inorganic counterparts, organic materials with strongly bounded electron-hole pair (excitons) require external driving force for excitons separation and charge generation. So, such a model with intermixed domains also presents extended interfacial area between the blended photoactive nanophases for bulk separation of photo generated excitons [1]. The photoactive blend of poly(3-hexylthiophene) (P3HT) donor and [6, 6]-phenyl C₆₁-butyric acid methyl ester (PCBM) acceptor has been one of the most interesting systems proposed for photocurrent generation. In the recent past, there has been a great boost in the efficiency of OSC utilizing this donor-acceptor mixture in the photoactive layer [2]. One of the key parameters that is under continuous investigation is the morphology transformation in this donor-acceptor pair with the changes in processing parameters for further possible improvements in the performance of devices prepared thereof. Optimum morphology pertaining to the donor-acceptor pair is the one where there is steady equilibrium between the crystallinity (molecular ordering) within each phase and nanoscale phase separation between intermixed domains [3, 4]. Definite order in the donor and acceptor moieties is responsible for photo absorption and carrier mobility. And, bi-continuous interphases in between the nanoscale donor-acceptor interpenetrating domains provide successful exciton dissociation and bi-directional pathways for carriers transport to their analogous electrodes [5].

Solution processing practice for active layer preparation in OSC allows manipulation over several parameters

including blending ratios of the two components, solvent system employed, post treatments such as thermal and solvent annealing etc., for modifying the photoactive layer morphology [6]. Though, post treatment methods such as solvent vapour annealing and thermal annealing have been doing well to improve the morphology and hence, the efficiency in OSCs. However, such methods may not prove to be effective for large scale manufacturing practice. On the other hand, solvent system employed for preparing active layer spin coating solution has an immense effect on the morphology of the thin film casted thereof. Earlier practice was to have a single solvent dissolving both the components of the blend. Such a system though may seem simple in practice however, is associated with the complications of interference from one component in the crystallisation process of the other component in the blend. And since, different materials have different solubility in a particular solvent, so single solvent may not be sufficient to serve the desired purpose.

Recently, solvent-co-solvent mixture approach has been successfully adopted to get the desired morphology. In such an approach, apart from the main solvent dissolving both the components equally, second solvent is introduced which offers limited solubility to one of the component (predominantly P3HT component) [7]. Accordingly, this solvent-non-solvent system can keep the PCBM well dissolved in the solution mixture so, that undissolved P3HT chains start to crystallise first in the solution itself without being interfered by the completely dissolved component (PCBM). So far, this approach of solvent-non-solvent mixture has been put to practice for modifying the morphology of the active layer in normal OSCs [8]. However, declining future of the normal architecture in OSCs due to its instability and degradation from oxygen

and moisture of the atmosphere shifted the interest towards its inverted configuration. This instability is caused by the presence of low work function reactive metal like aluminium at the top interfacing with the air in the normal architecture. Replacement of low work function metal by a high work function metal like silver (Ag) or gold (Au) can act to stabilize the system as a whole from the detrimental effect of moisture or air [9]. **Fig. 1** represents layer sequence in inverted configuration of OSC.

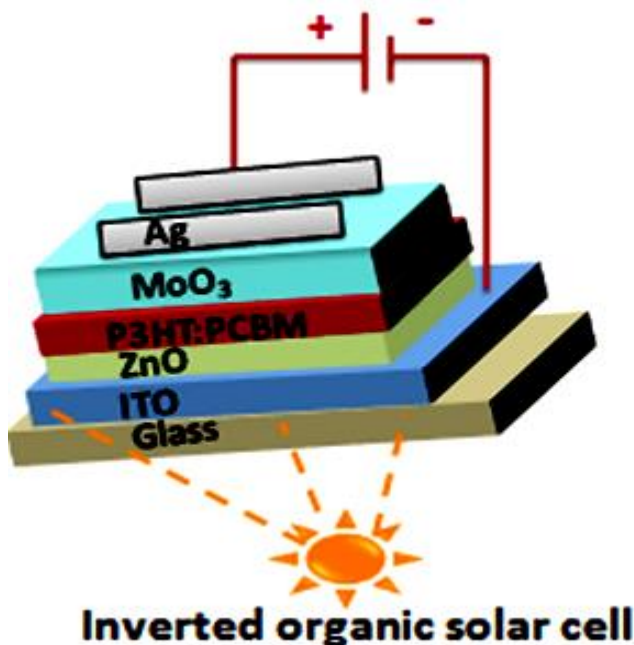


Fig. 1. Schematic illustration of the layer sequence in inverted configuration of organic solar cell.

We considered studying in detail the co-solvent addition during the preparation of active layer in inverted OSCs. The effect of co-solvent addition on the parameters crucial to device performance was studied. Solvent-cosolvent mixture method works by dissolving one component (mostly PCBM) of the blended mixture, avoiding interference of this component in the crystallisation process of the other component (i.e., P3HT donor polymer). As, there have been very limited studies on morphological modification of the active layer in inverted OSC via solvent mixture approach so, we considered carrying out a comprehensive study on the effect of ortho-dichlorobenzene (o-DCB)-cyclohexanone (CHN) solvent mixture on P3HT-PCBM layer in inverted OSC. This effect is worth studying, as the underlying and overlying layers positioned with the active layer in inverted configuration will cause the P3HT-PCBM mixture to behave differently from that of the normal OSCs to the solvent mixture modification.

Experimental

Materials

Poly(3-hexylthiophene) (P3HT) polymer and [6, 6]-phenyl C₆₁-butyric acid methyl ester (PCBM) were acquired of Sigma Aldrich. Solvents ortho-dichlorobenzene (o-DCB) and cyclohexanone (CHN) used in this study were of

analytical research grade and were also obtained from Sigma Aldrich. Indium tin oxide (ITO) coated glass substrates (5 × 5 cm sizes) with sheet resistance of less than 20 Ω/sq were obtained from Moserbaer India Ltd. Zinc acetate dihydrate, ethanolamine and 2-methoxyethanol for zinc oxide (ZnO) preparation also from Sigma Aldrich were used as received. Molybdenum oxide (MoO₃) and silver (Ag) wire were purchased from Central Drug House (CDH).

Methods

Constituent layer structure in inverted polymer solar cells comprises of ITO/ ZnO/ P3HT: PCBM/MoO₃/Ag. ITO coated glass substrates were first patterned using a diode-pumped Q-switch neodymium-doped yttrium aluminium garnet (Nd:Y₃Al₅O₁₂, Nd:YAG) laser scribe at its fundamental wavelength (λ=1047nm) and laser power of 1.0 W and cleaned thereafter via ultrasonication for 20 min each in a soap solution at 50 °C, demineralised water, acetone and isopropanol in succession. The cleaned substrates were then dried using nitrogen and treated further for 26 min in an UV-ozone chamber. Firstly, a ZnO (30 nm) layer was deposited on ITO using a 0.50M ZnO solution prepared by mixing (0.46 g) zinc acetate dihydrate with ethanolamine (stabilizer) and 2-methoxyethanol (solvent). Subsequent curing of the deposited ZnO layer was carried out at 250 °C for 10 min in air. Active layer spin coating solution was prepared by dissolving 18.7 mg of P3HT polymer and 11.3 mg of PCBM in 1 ml of good solvent i.e., o-DCB by means of stirring overnight at 50 °C on a hot plate. For active layer modification, cyclohexanone (CHN) co-solvent (5 volume %) was added to the above prepared active layer spin coating solution and stirred further for 2 h. Active layer (140 ± 10 nm thick) was then spin coated at 600 rpm for 2 min using this solution and deposited layer was cured at 85 °C for 30 min. Thereafter, 7 nm thick molybdenum oxide (MoO₃) and 150 nm thick silver (Ag) layers were thermally deposited at a deposition rate of 0.5 Å s⁻¹ and 1.0 Å s⁻¹ respectively, in a vacuum chamber maintained at a base pressure of 5 × 10⁻⁶ mbar. Final photovoltaic devices with an active area of 0.09 cm² were prepared with and without co-solvent modification in the active layer. And, a comparison of the performance of these devices with and without co-solvent modification was made.

Measurements

Device preparation was carried out in the nitrogen environment within a glove box from Jacomex with ΔP = 3.0 mbar & oxygen level of 0.3 ppm. The current density (J)–voltage (V) characteristics of the photovoltaic devices were measured using a Keithley Model 2420 source meter under a solar simulator (Model SS150AAA Photo Emission Technology Inc.) equipped with AM 1.5 G filter and with an illumination intensity of 100 mW cm⁻². The UV–visible absorption measurements were carried out using a Perkin Elmer lambda 35 UV–visible spectrophotometer. Surface morphology studies were done using atomic force microscope (AFM), VEECO DI-3100, with Nanoscope (III) in tapping mode. Grazing incidence X-ray diffraction (GI-XRD) measurements were done using Rigaku ultima IV X-ray diffractometer (λ=1.54 Å) with

Cu-K α radiation source at grazing incidence angles of 0.11° and 0.3° .

Results and discussion

Effect of ageing of precursor solution

P3HT:PCBM blend solution in solvent-non solvent mixture was known to undergo P3HT aggregation in a way similar to pure P3HT bulk solution in a non-solvent or marginal solvent. The aggregation of P3HT is known to take place by transition of P3HT from coil to extended rod owing to its solvophobic interaction with a marginal solvent followed by π - π stacking of the extended chains [10]. Aggregation can be stated in terms of disordered to ordered transformation of crystallising P3HT chains in a marginal solvent. Co-solvent used in our case is cyclohexanone solvent (CHN). CHN solvent is a marginal solvent for P3HT offering limited or lesser solubility to P3HT chains and more solubility to PCBM aggregates. Aggregation kinetics of P3HT in P3HT-PCBM blend solution in o-DCB-CHN solvent will be different from the aggregation of P3HT chains in pure P3HT bulk solution due to interference from the dissolved PCBM portions in the former [11]. Such an aggregation in P3HT-PCBM solution on marginal solvent addition is marked by increased absorption and enhanced P3HT crystallinity with subsequent changes in the colour of the solution from orange to purple. This process of aggregation is more recognizable with ageing i.e., storing the solution for a sufficient time at room temperature, manifested by increased viscosity and darkening of solution colour due to increasing amount of non-dissolved P3HT portions in the solution [12]. However, longer ageing and higher percentage of co-solvent can bring about gelling of the solution thus, making the solution incompatible for the spin coating operation [13]. So, an optimisation of the ageing phase and co-solvent amount is prerequisite for successful preparation of the active layer.

The absorption spectra of P3HT-PCBM films casted from o-DCB-CHN solvent mixture aged for various time was observed (Fig. 2a) for evaluating the dependence of ageing time on aggregation and subsequent absorption improvements. The absorption spectra of the films were characterized by a main peak around 512 nm, with two “shoulders” towards the higher wavelength region. The main peak is the characteristic of intrachain transitions in P3HT chains promoting decreased chain entanglement. Absorption shoulders towards higher wavelength are related to extended chain length absorption and interchain lamella stacking [14]. With ageing, these spectral features were found to be more pronounced. From the absorption spectra, it's been clear that there is considerable improvement in absorption with ageing for 1 h to 4 h at room temperature indicating evolution of ordered P3HT structures with ageing. However, a decrease in the absorption was noticed in the solution aged for 5 h possibly due to larger aggregate formation with no more advancement towards P3HT ordered arrangement [15]. Again, the difference in absorption intensity between 2, 3 and 4 h aged solution was modest. So, for our study we optimised the ageing period to 2 h, as longer treatment time

may not be a feasible idea for large scale production practice.

To gain better insight on the effect of ageing and crystallinity improvement upon ageing, grazing incidence X-ray diffraction (GI-XRD) measurements were carried out for P3HT-PCBM films at a grazing incidence angle of 0.3° (Fig. 2b). GI-XRD can provide valuable information about the crystallinity of P3HT in the blend film. A relative indication of crystallinity in P3HT:PCBM films casted from precursor solution aged for different times (1-5 h) was analysed by comparing the (100) reflection peak intensities observed at 2θ value of 5.426° . 2 h aged precursor solution with highest (100) peak intensity signifies most ordered P3HT arrangements [16]. Also, equally intense higher order diffractions in films prepared from 2h aged solution suggest higher crystallinity and self organisation ability in the blend film. So, aging time could be used as a management control towards attaining highly oriented crystals of P3HT in P3HT-PCBM blend films via solvent mixture approach. Such a molecularly ordered film of P3HT-PCBM can be taken advantage of, as an active layer of OSCs.

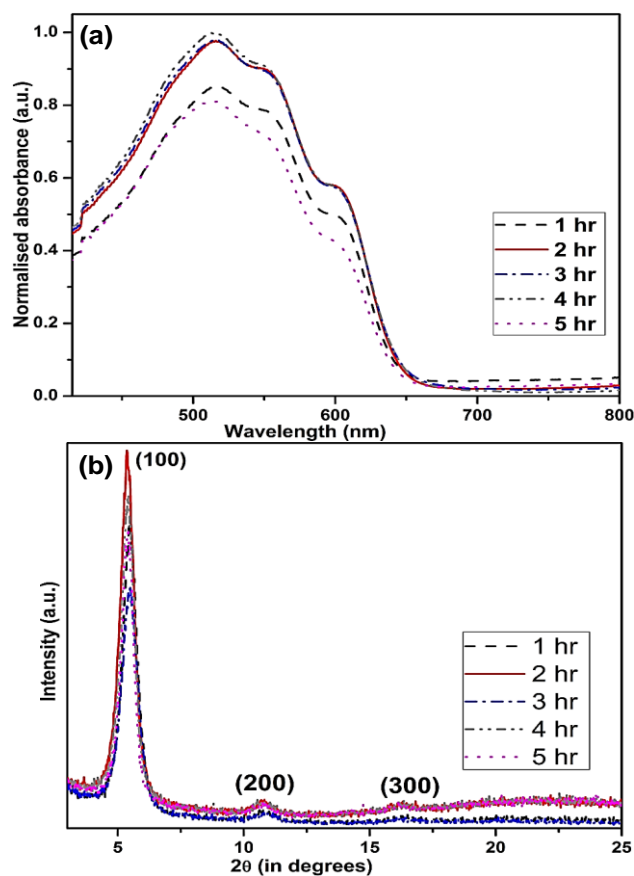


Fig. 2. (a) Absorption spectra of P3HT-PCBM films casted of precursor solutions aged for different times in o-DCB-CHN mixture (b) Out of plane GI-XRD patterns for P3HT-PCBM films casted of precursor solutions aged for different times in o-DCB-CHN mixture.

Again, the amount of marginal solvent was also optimised to be 5 volume %. As, lesser amount than this could not bring about significant crystallisation in the blend film. And also, larger amount of the CHN co-solvent would result in greater non-dissolved P3HT crystallites in the

precursor solution and subsequent gelling of the solution on keeping the same for few hours. So, using the optimised ageing time (2 h) and co-solvent amount (5 volume %), the effect of introducing this modified P3HT-PCBM layer as active layer in inverted OSC was further considered.

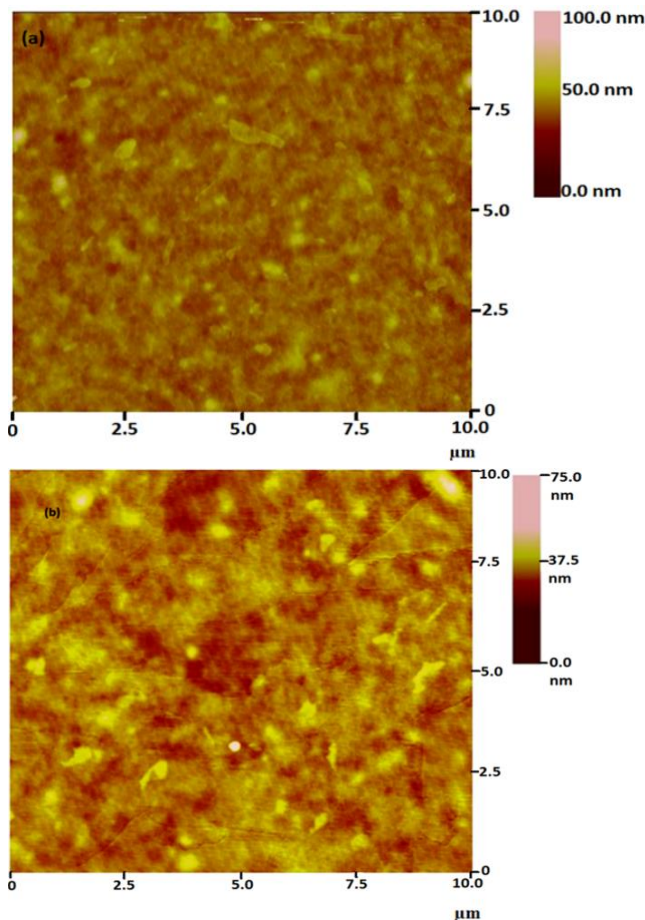


Fig. 3. Tapping mode AFM image scans ($10 \times 10 \mu\text{m}$) of P3HT:PCBM films (a) Without any modification (b) with CHN modification.

Morphological characterization

Morphological studies of P3HT-PCBM layer casted with and without CHN addition was carried out using tapping mode atomic force microscopy (AFM). **Fig. 3 a, b** shows the topographical AFM image of P3HT-PCBM film without any modification and with CHN modification, respectively. Surface images show significant dependence of film morphology on the solvent mixture used to dissolve the blend materials. In a conventional film with single good solvent (o-DCB) dissolving both the components of the mixture, no clear separation between P3HT (brighter region) and PCBM (darker regions) phases was noticeable. Such a homogenous feature all through the conventional film could possibly be resulting from co-precipitation of both components from the mixture at the same time. However, with CHN addition, the extent of phase separation between two components seems to be improved. Such a phase separation could be a result of preferential crystallisation and aggregation of P3HT component directing further demixing of the phases on spin casting and subsequent annealing [17]. Such a lateral phase separation between the components of the blend at all depths of the

film is required for efficient dissociation of the photoinduced exciton for charge generation. So, CHN addition seems to be beneficial in giving the blend film the desired morphology.

UV-visible absorption measurements

The analysis of absorption spectra of P3HT-PCBM films in the visible range was carried out to see the effect of CHN addition on the relative light absorption properties and crystal structure arrangement of P3HT chains in the active layer. **Fig. 4** shows the comparative UV-visible absorption spectrum of P3HT-PCBM layer spin coated from a solution with and without CHN modification. As discussed previously, absorption spectra show one main peak around 512 nm and two absorption shoulders in the lower energy region corresponding to absorption by the highly organized solid P3HT aggregates. Upon CHN addition, a slight shift in the peak to higher wavelength side and an equivalent increase in intensities of main absorption peak and low energy vibronic bands were observed. Absorption spectrum of the modified film reveals growth of more well ordered P3HT crystals. This well controlled growth in P3HT crystals is supported by coil to extended rod spontaneous transition induced by decreased polymer-poor solvent interaction. This transformation follows on to aggregation in polymer domains by stronger π - π interaction set among these extended P3HT chains [18]. However, in a conventional P3HT-PCBM film casted of a single good solvent (o-DCB), such a transformation is not very feasible due to well dissolved P3HT chains in o-DCB.

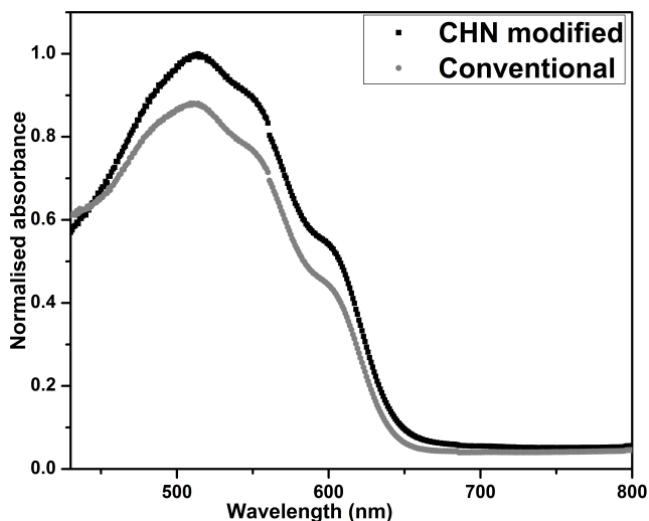


Fig. 4. Absorption spectra of P3HT-PCBM films with and without co-solvent modification.

Grazing incidence x-ray diffraction (GI-XRD) measurements

To substantiate the effect of CHN addition on the crystalline structure and molecular ordering in the active layer of inverted OSC, GI-XRD measurements were carried out on spin coated films of P3HT-PCBM. For outlining the structural characteristics through the depth profiling of the P3HT-PCBM thin film, GI-XRD measurements were carried out at two grazing incidence angles. Considering some recent papers reporting GIXRD measurements using

lab instruments for stronger scattering films, we determined on carrying out depth profiling of the P3HT-PCBM thin film with our laboratory source GI-XRD instrument [19]. At grazing incidence angle less than the critical angle for P3HT-PCBM film (i.e., at 0.11°), total exterior reflection takes place with X-ray penetrating to merely ~ 10 - 12 nm underneath the surface of the film. So, diffraction patterns at 0.11° grazing incidence angle consist of reflections mainly occurring from the interlayer spacing between P3HT crystallites present at the surface of the film [20]. While, keeping incidence angle greater than the critical angle for P3HT-PCBM film and less than the critical angle of the substrate (i.e., at 0.3°), X-ray can be made to penetrate the entire thin film. So, at 0.3° grazing incidence angle, reflections from the whole bulk of the film can be obtained.

Fig. 5(a, b) depicts the X-ray diffractograms of the P3HT-PCBM film at two grazing incidence angles 0.11° and 0.3° , respectively. Interlayer distances (d) and crystallite sizes of P3HT domains calculated of the (100) diffraction peaks are given in Table 1. Crystallite sizes are calculated using the Scherrer's formula via taking in to account the peak broadening in the corresponding diffraction patterns.

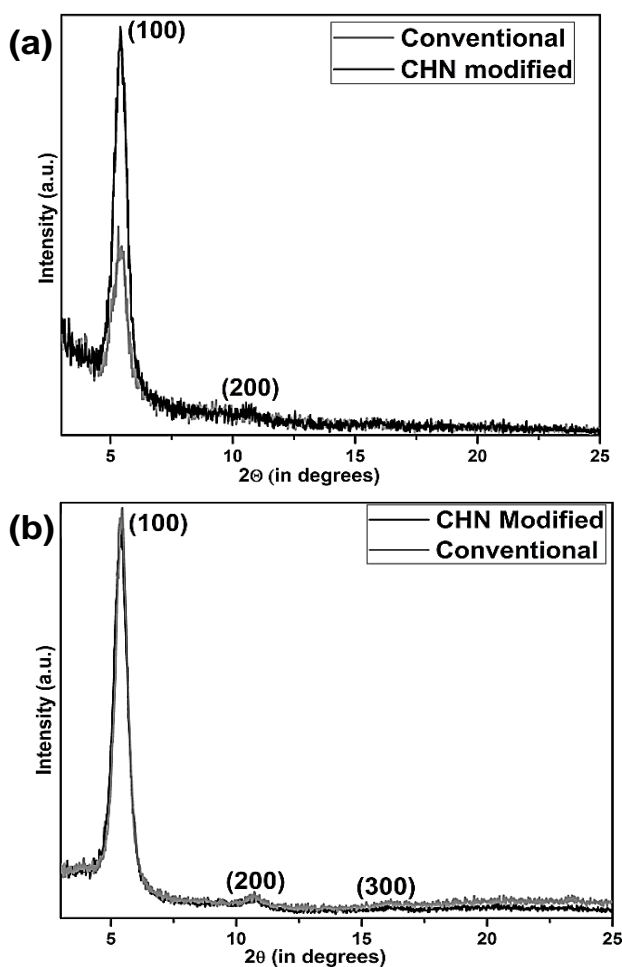


Fig. 5. (a) Grazing incidence X-ray diffraction (GI-XRD) profiles of P3HT:PCBM composite films with and without CHN modification at grazing incidence of 0.11° (b) GI-XRD profiles of films at grazing incidence of 0.3° .

$T = K\lambda/\beta \cos \theta$ where, β = full width half maximum (FWHM), λ = wavelength of X-ray (1.54 \AA) and T = crystallite size. Both the diffractograms mainly show three peaks corresponding to reflections from (100), (200) and (300) axis orientation of lamellar P3HT chains [21].

Table 1. Summary of interlayer distances (d) and the size of P3HT crystallites determined of the (100) diffraction peak at two grazing incidences 0.11° and 0.3° in the XRD pattern.

S.No.	Device	Grazing incidence angle (degree)	2θ value (degree)	Interlayer distance d_{100} (Å)	FWHM	Grain size (nm)
1.	Cyclohexanone modified	0.11°	5.4	16.27	0.608	13.0
2.	Cyclohexanone modified	0.3°	5.3	16.48	0.654	12.02
3.	Conventional	0.11°	5.4	16.29	0.654	12.03
4.	Conventional	0.3°	5.4	16.37	0.585	13.44

A comparison of the (100) reflection peak intensities at 0.11° grazing incidence angle from unmodified and CHN modified P3HT-PCBM films were done to analyse the crystalline characteristic of P3HT phase at the film surface. An increase in the intensity of (100) reflection peak observed at $2\theta = 5.426^\circ$ in the CHN modified film as compared to unmodified film signifies higher level of ordering and orientation of P3HT chains at the surface of the film upon CHN addition. However, much difference was not noted in the higher order diffraction peaks of the two films or these peaks were very less pronounced as only a transient beam of X-ray was made to fall on a smaller depth of P3HT-PCBM film at 0.11° incidence. A comparison of the crystallite sizes and interlayer spacing between P3HT chains reveals larger well developed closely spaced P3HT crystallites in CHN modified sample as compared to limitedly crystallised smaller crystallites at the surface of unmodified sample. The reason for such a distinctive feature observed with mixed solvent approach is associated with the CHN (poor solvent for P3HT) induced preferential self assembly of P3HT in the good solvent-poor solvent mixture [22].

Again, a comparison of (100) diffraction peak intensity at grazing incidence angle of 0.3° revealed slightly more number of better crystallised P3HT domains in the bulk of conventional unmodified film as compared to CHN modified P3HT-PCBM film. Higher order diffraction peaks (200) and (300) were also more pronounced in the bulk of the conventional unmodified sample than the CHN modified sample. As, the blend films with the identical thickness and concentration have same number of P3HT chains so, it can be stated that solvent-non solvent mixture method not only brings about the preferential crystallisation of P3HT domains but also, stimulates upward distribution of P3HT fractions. Although, it is known that in a solution processing technique such as spin coating the P3HT fractions with the lower surface energy factor have a tendency to occupy surface of the film [23]. Such a probability is however, found to be more enhanced with the practice of solvent-non solvent mixture for spin coating. This vertical concentration gradient in the blend film with CHN modification must benefit the inverted device prepared thereof with the modified P3HT-PCBM layer being employed as active layer for photoabsorption. As more crystallised P3HT domains occupy the surface of the active layer in contact with the MoO_3 (hole transporting

layer, HTL) layer with CHN modification, hole transport to the silver anode would be enhanced. In addition, leakage current due to wrong carrier ion transport to anode would be minimised. GI-XRD measurement thus confirms favourable vertical concentration gradient of P3HT fractions with CHN addition.

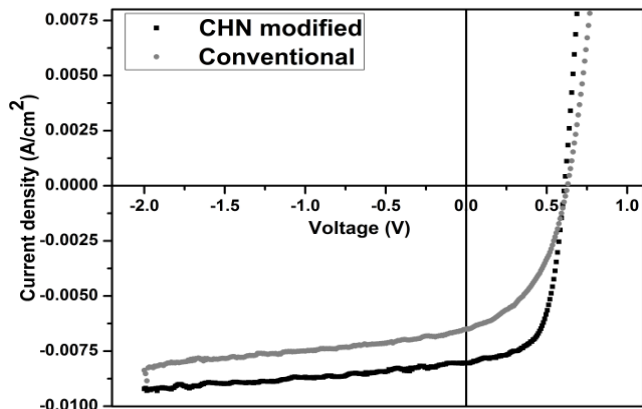


Fig. 6. Current density-voltage (J - V) characteristic of devices fabricated with and without co-solvent modification in the active layer under AM 1.5 G white light illumination.

Photovoltaic characteristics

We then fabricated an inverted device with layer sequence of Glass/ITO/ZnO/P3HT-PCBM/MoO₃/Ag, to consider the effect of CHN addition to the active layer spin coating solution on the photovoltaic characteristic of the prepared device. Each photovoltaic device consists of four cells each with an active area of 0.09 cm² and device properties were measured under an illumination intensity of 100 mW cm⁻², AM 1.5 G condition. **Fig. 6** compares the current density-voltage (J - V) characteristics of the devices prepared with and without CHN modification to the active layer spin coating solution. Photovoltaic parameters of the as prepared inverted devices are summarised in **Table 2**.

Table 2. Summary of photovoltaic device parameters for ITO/ZnO/P3HT: PCBM/MoO₃/Ag polymer solar cell under AM 1.5 G white light illumination, with and without CHN modification in the active layer preparation.

^b Substrate	Cell No.	Device	V_{oc} (V)	J_{sc} (Acm ⁻²)	FF	%E	R_{sh} (Ω cm ²)	R_s (Ω cm ²)
1	1	^a cyclohexanone modified	0.61	8.04E-03	0.61	3.01	700	12
1	2	cyclohexanone modified	0.61	8.14E-03	0.62	3.09	600	12
1	3	cyclohexanone modified	0.62	7.94E-03	0.61	3.00	1167	12
1	4	cyclohexanone modified	0.62	7.62E-03	0.64	3.01	1391	12
2	1	^a Conventional	0.61	7.41E-03	0.61	2.77	1123	14
2	2	Conventional	0.61	7.66E-03	0.58	2.72	634	15
2	3	Conventional	0.61	7.45E-03	0.60	2.74	489	13
2	4	Conventional	0.62	7.28E-03	0.60	2.69	654	14

^aConventional device = Device prepared with active layer casted from a good solvent (O-DCB).

Cyclohexanone modified= Device prepared with active layer modified by cyclohexanone addition

^bSubstrate is a 5cm × 5cm ITO glass substrate with inverted cell layer sequence comprising 4 cells each of area 0.09 cm².

It can be observed that conventional photovoltaic device fabricated with active layer casted from a single good solvent showed a power conversion efficiency (PCE) of 2.77% resulting from the short circuit current density (J_{sc}) of 7.41E-03 A cm⁻², open circuit voltage (V_{oc}) of 0.61 V and fill factor (FF) of 0.61. However, o-DCB-CHN mixed

solvent casted active layer in a typical inverted device could result in a PCE of 3.09% with a J_{sc} value of 8.14E-03 A cm⁻², V_{oc} of 0.61V and FF of 0.62. The resulting increase in efficiency from 2.77% to 3.09% with the addition of poor solvent (CHN) to the main solvent (o-DCB) during the preparation of active layer precursor solution could possibly be due to the increase in the photocurrent generation and increasing fill factor of the device. Improved crystallisation in the polymer donor domains evident of the UV-vis and GI-XRD measurements could be the reason for realising increased current density in the modified devices [24].

Favourable upright concentration gradient must have brought about the observed increase in the FF of the device. As the fractions of P3HT close to the HTL layer increases, series resistance in the device decreases and smoother efficient pathway for hole transport must be set in. So, CHN addition in the active layer preparation of inverted OSC benefits the device prepared thereof in two ways. Firstly, by improved crystallisation of the donor polymer for enhanced photo absorption and hole transport and secondly, by setting up a favourable upright concentration gradient in the active layer with better crystallised P3HT at the top in close contact with HTL for efficient hole transport to anode.

Conclusion

This work described the optimisation of amount of non-solvent added and ageing period of the precursor solution for obtaining the best possible crystallisation in the donor phase. Increasing the ordering in the precursor solution by addition of poor solvent (cyclohexanone) enhances appreciably the crystallinity and order in the P3HT-PCBM films compared with films prepared from disordered precursor solution. Practice of the CHN modified P3HT-PCBM film as active layer of inverted OSC improves the PCE to a value of 3.09% as compared to 2.77% in the unmodified device. This improvement was related to the increased current density and fill factor of the device with CHN addition. Characteristics of well ordered donor phase in the active layer and favourable concentration gradient with encouraging distribution of donor domains closer to hole transport layer are introduced to the inverted OSC via CHN addition.

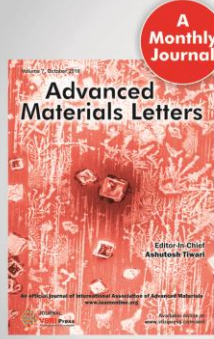
Acknowledgements

Authors are thankful to Prof. Pradeep kumar, Vice-Chancellor, Delhi Technological University, Delhi for encouragement and support. A financial support to one of the author, Sarita is also acknowledged gratefully. The authors are also grateful to Moserbaer India Ltd. for their assistance in performing the experiment and characterization.

References

- Halls, J.J.M.; Walsh, C.A.; Marseglia, E.A.; Friend, R.H.; Moratti, S.C. and Holmes, A.B., *Nature*, **1995**, 376, 498.
DOI: [10.1038/376498a0](https://doi.org/10.1038/376498a0)
- Thompson, B.C. and Frechet, J.M.J., *Angew Chem. Int. Ed.*, **2008**, 47, 58.
DOI: [10.1002/anie.200702506](https://doi.org/10.1002/anie.200702506)
- Chen, L.-M.; Hong, Z.; Li, G. and Yang, Y., *Adv. Mater.*, **2009**, 21, 1434.
DOI: [10.1002/adma.200802854](https://doi.org/10.1002/adma.200802854)
- Wang, Y.; Wei, W.; Liu, X. and Gu, Y., *Sol. Energy Mater. Sol. Cells*, **2012**, 98, 129.
DOI: [10.1016/j.solmat.2011.10.003](https://doi.org/10.1016/j.solmat.2011.10.003)

5. Hoppe, H.; Niggemann, M.; Winder, C.; Kraut, J.; Hiesgen, R.; Hinsch, A.; Meissner, D. and Sariciftci, N.S., *Adv. Funct. Mater.*, **2004**, *14*, 1005.
DOI: [10.1002/adfm.200305026](https://doi.org/10.1002/adfm.200305026)
6. Li, G.; Shrotriya, V.; Yao, Y.; Huang, J. and Yang, Y., *J. Mater. Chem.*, **2007**, *17*, 3126.
DOI: [10.1039/B703075B](https://doi.org/10.1039/B703075B)
7. Reisdorffer, F.; Haas, O.; Le Rendu, P. and Nguyen, T.P., *Synth. Met.*, **2012**, *161*, 2544.
DOI: [10.1016/j.synthmet.2011.08.005](https://doi.org/10.1016/j.synthmet.2011.08.005)
8. Yusli, M.N.; Yun, T.W. and Sulaiman, K., *Mater. Lett.*, **2009**, *63*, 2691.
DOI: [10.1016/j.matlet.2009.09.044](https://doi.org/10.1016/j.matlet.2009.09.044)
9. Zhang, F.; Xu, X.; Tang, W.; Zhang, J.; Zhuo, Z.; Wang, J.; Wang, J.; Xu, Z. and Wang, Y., *Sol. Energy Mater. Sol. Cells*, **2011**, *95*, 1785.
DOI: [10.1016/j.solmat.2011.02.002](https://doi.org/10.1016/j.solmat.2011.02.002)
10. Xu, W.; Li, L.; Tang, H.; Li, H.; Zhao, X. and Yang, X., *J. Phys. Chem. B*, **2011**, *115*, 6412.
DOI: [10.1021/jp201044b](https://doi.org/10.1021/jp201044b)
11. Liu, J.; Shao, S.; Wang, H.; Zhao, K.; Xue, L.; Gao, X.; Xie, Z. and Han, Y., *Org. Electron.*, **2010**, *11*, 775.
DOI: [10.1016/j.orgel.2010.01.017](https://doi.org/10.1016/j.orgel.2010.01.017)
12. Bielecka, U.; Lutsyk, P.; Janus, K.; Sworakowski, J. and Bartkowiak, W., *Org. Electron.*, **2011**, *12*, 1768.
DOI: [10.1016/j.orgel.2011.06.027](https://doi.org/10.1016/j.orgel.2011.06.027)
13. Huang, W.Y.; Huang, P.T.; Han, Y.K.; Lee, C.C.; Hsieh, T.L. and Chang, M.Y., *Macromolecules*, **2008**, *41*, 7485.
DOI: [10.1021/ma801368z](https://doi.org/10.1021/ma801368z)
14. Kim, J.S.; Lee, J.H.; Park, J.H.; Shim, C.; Sim, M. and Cho, K., *Adv. Funct. Mater.*, **2011**, *21*, 480.
DOI: [10.1002/adfm.201000971](https://doi.org/10.1002/adfm.201000971)
15. Park, Y.D.; Lee, S.G.; Lee, H.S.; Kwak, D.; Lee, D.H. and Cho, K., *J. Mater. Chem.*, **2011**, *21*, 2338.
DOI: [10.1039/C0JM03114C](https://doi.org/10.1039/C0JM03114C)
16. Jeon, J.H.; Lee, H.K.; Wang, D.H.; Park, J.H. and Park, O.O., *Sol. Energy Mater. Sol. Cells*, **2012**, *102*, 196.
DOI: [10.1016/j.solmat.2012.03.002](https://doi.org/10.1016/j.solmat.2012.03.002)
17. Li, L.; Tang, H.; Wu, H.; Lu, G. and Yang, X., *Org Electron*, **2009**, *10*, 1334.
DOI: [10.1016/j.orgel.2009.07.016](https://doi.org/10.1016/j.orgel.2009.07.016)
18. Moulé, A.J. and Meerholz, K., *Adv. Mater.*, **2008**, *20*, 240.
DOI: [10.1002/adma.200701519](https://doi.org/10.1002/adma.200701519)
19. Gundlach, D.J.; Royer, J.E.; Park, S.K.; Subramanian, S.; Jurchescu, O.D.; Hamadani, B.H.; Moad, A.J.; Kline, R.J.; et al., *Nat. Mater.*, **2008**, *7*, 216.
DOI: [10.1038/nmat2122](https://doi.org/10.1038/nmat2122)
20. Treat, N.D.; Brady, M.A.; Smith, G.; Toney, M.F.; Kramer, E.J.; Hawker, C.J. and Chabinyc, M.L., *Adv. Energy Mater.*, **2011**, *1*, 82.
DOI: [10.1002/aenm.201000023](https://doi.org/10.1002/aenm.201000023)
21. Chen, F.-C.; Ko, C.-J.; Wu, J.-L. and Chen, W.-C., *Sol. Energy Mater. Sol. Cells*, **2010**, *94*, 2426.
DOI: [10.1016/j.solmat.2010.09.004](https://doi.org/10.1016/j.solmat.2010.09.004)
22. Park, Y.D.; Lee, H.S.; Choi, Y.J.; Kwak, D.; Cho, J.H.; Lee, S. and Cho, K., *Adv. Funct. Mater.*, **2009**, *19*, 1200.
DOI: [10.1002/adfm.200801763](https://doi.org/10.1002/adfm.200801763)
23. Karagiannidis, P.G.; Georgiou, D.; Pitsalidis, C.; Laskarakis, A. and Logothetidis, S., *Mater. Chem. Phys.*, **2011**, *129*, 1207.
DOI: [10.1016/j.matchemphys.2011.06.007](https://doi.org/10.1016/j.matchemphys.2011.06.007)
24. Zhao, Y.; Shao, S.; Xie, Z.; Geng, Y. and Wang, L., *J. Phys. Chem. C*, **2009**, *113*, 17235.
DOI: [10.1021/jp9038286](https://doi.org/10.1021/jp9038286)




Copyright © 2016 VBRI Press AB, Sweden

A Monthly Journal

Publish your article in this journal

Advanced Materials Letters is an official international journal of International Association of Advanced Materials (IAAM, www.iaamonline.org) published monthly by VBRI Press AB from Sweden. The journal is intended to provide high-quality peer-review articles in the fascinating field of materials science and technology particularly in the area of structure, synthesis and processing, characterisation, advanced-state properties and applications of materials. All published articles are indexed in various databases and are available download for free. The manuscript management system is completely electronic and has fast and fair peer-review process. The journal includes review article, research article, notes, letter to editor and short communications.

www.vbripress.com/aml



VBRI Press
Commitment to Excellence